JVI Journals.ASM.org

Epstein-Barr Virus-Encoded Latent Membrane Protein 2A Promotes the Epithelial-Mesenchymal Transition in Nasopharyngeal Carcinoma via Metastatic Tumor Antigen 1 and Mechanistic Target of Rapamycin Signaling Induction

Zhe Lin,[a] Xin Wan,[a] Runqiu Jiang,[b] Lei Deng,[b] Yun Gao,[b] Junwei Tang,[b] Yu Yang,[b] Wei Zhao,[a] Xin Yan,[a] Kun Yao,[a] Beicheng Sun,[b] Yun Chen[a]

Department of Microbiology and Immunology, Nanjing Medical University, Nanjing, Jiangsu Province, China[a]; Liver Transplantation Center, The First Affiliated Hospital of Nanjing Medical University, Nanjing, Jiangsu Province, China[b]

ABSTRACT

Epstein-Barr virus-encoded latent membrane protein 2A (LMP2A) promotes the epithelial-mesenchymal transition (EMT) of nasopharyngeal carcinoma (NPC), thereby increasing tumor invasion. Recently, the dysregulation of metastatic tumor antigen 1 (MTA1) was found to enhance tumor metastasis in a variety of cancers. A molecular connection between these two proteins has been proposed but not firmly established. In this study, we reported the overexpression of MTA1 in 29/60 (48.3%) NPC patients, and the overexpression of MTA1 significantly correlated with tumor metastasis. The overexpression of MTA1 promoted EMT via the Wnt1 pathway and β-catenin activation. We demonstrated that LMP2A reinforces the expression of MTA1 via the mechanistic target of rapamycin (mTOR) pathway to promote EMT in NPC. Furthermore, by knocking down 4EBP1 in combination with the new mTOR inhibitor INK-128 treatment, we discovered that LMP2A expression activates the 4EBP1-eIF4E axis and increases the expression of MTA1 at the translational level partially independent of c-myc. These findings provided novel insights into the correlation between the LMP2A and MTA1 proteins and reveal a novel function of the 4EBP1-eIF4E axis in EMT of nasopharyngeal carcinoma.

IMPORTANCE

Prevention of the recurrence and metastasis of NPC is critical to achieving a successful NPC treatment. As we all know, EMT has a vital role in metastasis of malignancies. LMP2A, an oncoprotein of Epstein-Barr virus, a well-known NPC activator, induces EMT and has been proved to exert a promoting effect in tumor metastasis. Our study demonstrated that LMP2A could induce EMT by activating MTA1 at the translational level via activating mTOR signaling and the 4EBP1-eIF4E axis. Taken together, our findings bridge the gap between the NPC-specific cell surface molecule and the final phenotype of the NPC cells. Additionally, our findings indicate that LMP2A and mTOR will serve as targets for NPC therapy in the future.

Nasopharyngeal carcinoma (NPC) is a head-and-neck tumor that occurs in the epithelial lining of the nasopharynx. The disease occurs with much greater frequency in southern China, northern Africa, and Alaska (1). Although NPC is sensitive to radio- and chemotherapy (2), high rates of local recurrence and distant metastasis dramatically compromise the effectiveness of these therapies (3, 4). Reducing the recurrence of tumors and preventing metastasis are critical to achieve a successful NPC treatment (5). Therefore, understanding the molecular mechanism of tumor metastasis appears to be very important. The epithelial-mesenchymal transition (EMT) was recently proposed to play a fundamental role in metastasis (6, 7). This transition allows tumor cells to acquire stem cell-like properties (8), thereby initiating tumor metastasis and recurrence (9).

Several tumor-specific antigens, including latent membrane protein 1 (LMP1) and latent membrane proteins 2A and 2B (LMP2A and LMP2B), are expressed on the surface of NPC cells (10). LMP2A has been shown to play a role in promoting tumor metastasis (11, 12). LMP2A induces epithelial cell migration by activating endogenous Syk activity via tyrosine residues in the LMP2A tyrosine-based activation motif (13). LMP2A also induces EMT and stem cell-like self-renewal in NPC, suggesting a mechanism by which Epstein-Barr virus (EBV) induces the initiation, metastasis, and recurrence of NPC (12). However, the molecular and mechanistic details of this transition remain unclear.

Recent studies suggest that the mechanistic target of rapamycin (mTOR) can be activated by overexpression of LMP2A in carcinoma cells (14). mTOR is a downstream serine/threonine kinase in the phosphatidylinositol 3-kinase (PI3K)/Akt pathway (15, 16), which integrates signals from the tumor microenvironment to regulation of multiple cellular processes (17, 18). The activation of the PI3K/Akt pathway in LMP2A-expressing NPC inhibits transforming growth factor β1 (TGF-β1)-induced apoptosis (19). A link between LMP2A expression, epithelial cell migration, and NPC metastasis may explain the high incidence of recurrence and metastasis in NPC progression (11, 20).

Received 28 June 2014 **Accepted** 14 July 2014

Published ahead of print 6 August 2014

Editor: R. M. Longnecker

Address correspondence to Yun Chen, chenyun@njmu.edu.cn, or Beicheng Sun, sunbc@njmu.edu.cn.

Copyright © 2014, American Society for Microbiology. All Rights Reserved.

doi:10.1128/JVI.01867-14

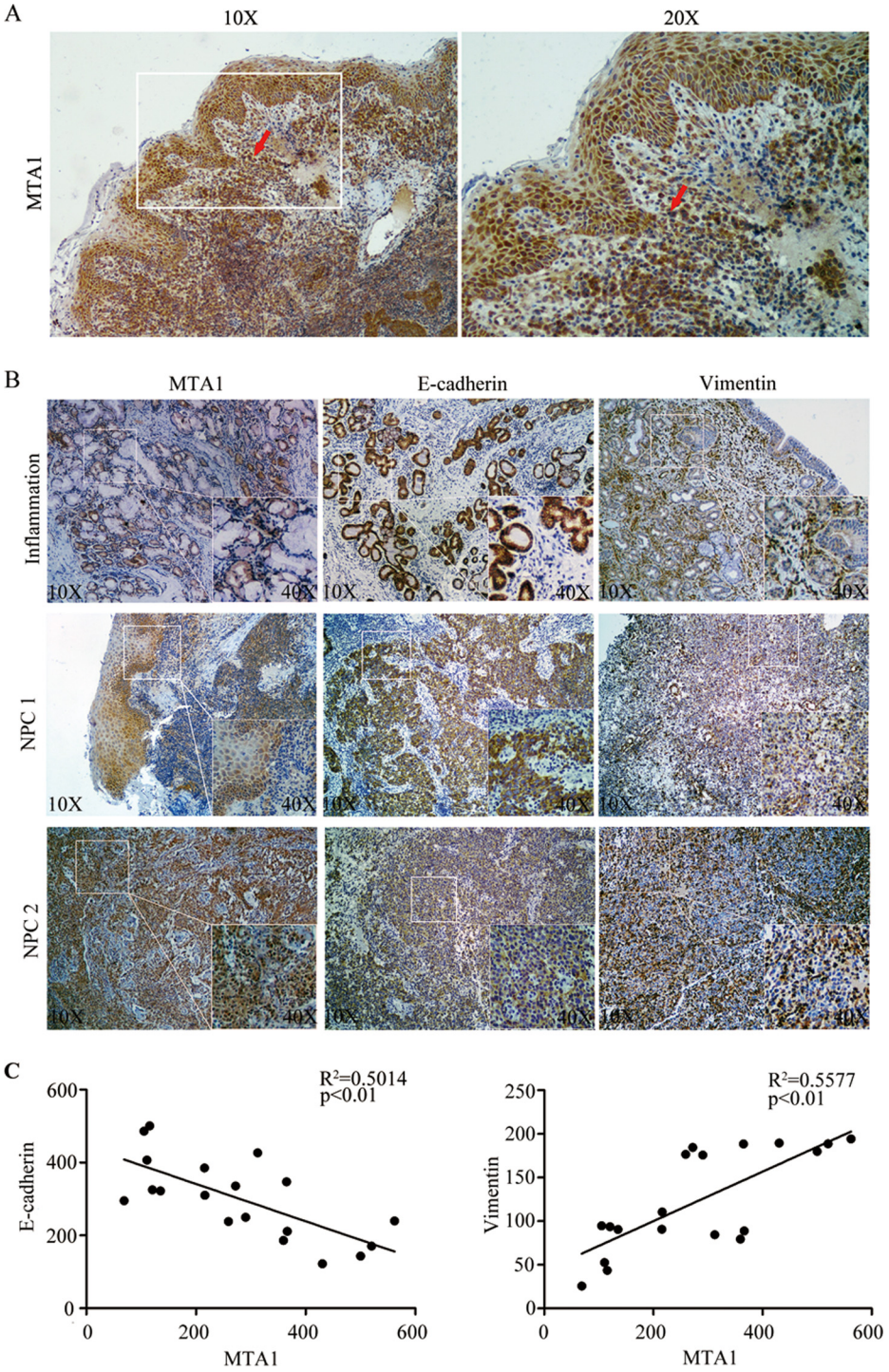

FIG 1 Expression of MTA1 correlates with tumor invasion and the expression of EMT markers in NPC. (A) Immunohistochemical analysis showing specific staining of MTA1 in NPC tumor squamous metaplasia and the breakthrough basement membrane (indicated by the red arrow). (B) The expression of MTA1, E-cadherin, and vimentin in inflammation and NPC tumor biopsy specimens as determined by immunohistochemical analysis. The inset shows images at a higher magnification. (C) The expression of MTA1 significantly correlates with E-cadherin and vimentin expression in NPC tissues. The coordinate axes are equal to the IOD means.

A novel metastasis-associated gene, metastatic tumor antigen 1 (MTA1), was identified to play an important role in tumor recurrence and metastasis (21). Overexpression of MTA1 in NPC positively correlates with TM (tumor metastasis) classification, clinical stage, distant metastasis, and death (22). The upregulation of MTA1 expression has been observed in breast cancer (23), prostate cancer (24), lung cancer (25), esophageal squamous cell carcinomas (26), gastrointestinal carcinoma (27), pancreatic cancer

(28), and invasive esophageal carcinomas (29). Many studies have reported that the occurrence of EMT may be induced by stimulating the expression of MTA1 (30–33). Recent studies have shown that mTOR is an important regulator of MTA1 (34), and many molecules in the mTOR signaling pathway regulate MTA1 expression (31, 35). In this study, we report a novel signaling pathway model in EBV-associated NPC. The expression of EBV LMP2A on the surface of NPC cells enhanced the capacity of NPC metastasis by upregulating the expression of MTA1. This upregulation is based on the activation of the mTOR and 4EBP1-eIF4E axis and nuclear translocation of β-catenin. The overexpression of LMP2A causes NPC cells to acquire metastatic characteristics and eventually increases the incidence of tumor recurrence and metastasis.

MATERIALS AND METHODS

Ethics statement. All animal work was conducted under the institutional guidelines of Jiangsu Province and approved by the Use Committee for Animal Care. Approval from the Nanjing Medical University Institute Research Ethics Committee was obtained, and written informed consent was provided by each human subject.

Lentivirus production and infection. LMP2A and MTA1 were subcloned into an HIV-1 lentiviral vector, pLV-GFP (gift from D. Trono, University of Geneva, Switzerland), by restriction digestion using BamHI and MluI (New England BioLabs, United Kingdom); the resulting constructs were called pLV-LMP2A and pLV-MTA1. The lentiviral pLL3.7-GFP vector (a gift from Kun Yao) was used to clone short hairpin RNA (shRNA) under the control of the mouse U6 promoter. The shRNA sequences were 5′-AACGAACATCTACGACATCTCCTTCAAGAGAGGA GATGTCGTAGATGTTCTTTTTTC-3′ (36) and 5′-AACTGGTTTACA TGTCGACTAATTCAAGAGATTAGTCGACATGTAAACCTTTTTT TC-3′ for MTA1 and scramble, respectively. All constructs were sequence verified. Details are available on request. Recombinant lentivirus was generated from 293T cells by cotransfection of pdelta-8.91 and pVSVG (a gift from Kun Yao) together with pLV-control, pLV-MTA1, pLV-LMP2A, pLL3.7-siMTA1, and pLL3.7-scramble. Green fluorescent protein (GFP) labels are used in these vectors, and green signal is produced when it is exposed to excitation light. The NPC cell lines CNE-1, CNE-2, and SUNE-1 were obtained from Sun Yat-Sen University, and CNE were obtained from the Chinese Academy of Sciences and maintained in RPMI 1640 medium (Life Technologies, Carlsbad, CA, USA) supplemented with 10% fetal bovine serum, 100 U/ml penicillin, and 100 μg/ml streptomycin (Invitrogen, Carlsbad, CA, USA) in a humidified 5% CO_2 incubator at 37°C. A pure population of infected cells was sorted based on GFP expression by flow cytometry; more than 98% of the cells were GFP positive after sorting. CNE-1-LMP2A$^+$MTA1$^-$ and CNE-2-LMP2A$^+$MTA1$^-$ cell lines with LMP2A gene stable expression but MTA1 gene knockdown were constructed as follows. First, GFP-positive CNE-1 and CNE-2 cells were sorted 3 days after being infected with lentiviral vectors expressing LMP2A and the control. The cells then were infected with lentiviral vectors expressing short interfering RNA (siRNA) of MTA1 (siMTA1) and scramble. However, LMP2A and MTA1 expression levels for the single-cell clones of the twice-infected cells were detected by using Western blotting, which was used to confirm the transfection efficiency of CNE-1-LMP2A$^+$MTA1$^-$ and CNE-2-LMP2A$^+$MTA1$^-$ cell lines.

RNA interference. siRNA specifically targeting c-myc, 4EBP1, and a corresponding scrambled siRNA control (Santa Cruz Biotechnology, Santa Cruz, CA, USA) were transfected into cells in 6-well plates using Lipofectamine 2000 reagent (Invitrogen, Carlsbad, CA, USA) according to the manufacturer's instructions. The gene silencing effect was tested by Western blotting at 48 h posttransfection.

Tissue samples. Paraffin-embedded NPC biopsy specimens from a total of 60 NPC patients and 10 inflammation controls (all adults who had been histologically and clinically diagnosed) were collected from the archives of the First Affiliated Hospital of Nanjing Medical University (Nanjing, China). Informed consent from the patients and approval from the Institute Research Ethics Committee were obtained prior to the study.

TABLE 1 Correlation between the expression of MTA1 and the clinicopathological characteristics of NPC patients[a]

Parameter[b]	No. of cases	MTA1 protein expression (no. of patients [%])		*P* value (chi-square test)
		Low expression	High expression	
Sex				0.46
Male	38	21 (55.3)	17 (44.7)	
Female	22	10 (45.5)	12 (54.5)	
Age (yr)				0.75
≤50	36	18 (50.0)	18 (50.0)	
>50	24	13 (54.2)	11 (45.8)	
T classification				0.13
T1-T2	33	20 (60.6)	13 (39.4)	
T3-T4	27	11 (40.7)	16 (59.3)	
N classification				<0.01
N0-N1	41	26 (63.4)	15 (36.6)	
N2-N3	19	5 (26.3)	14 (73.7)	
M classification				0.03
M0	43	26 (60.5)	17 (39.5)	
M1	17	5 (29.4)	12 (70.6)	
Clinical stage				0.06
I-II	26	17 (65.4)	9 (34.6)	
III-IV	34	14 (41.2)	20 (58.8)	
LMP2A				0.03
Positive	39	16 (41.0)	23 (59.0)	
Negative	21	15 (71.4)	6 (28.6)	

[a] Restaged according to the 7th edition of the UICC/AJCC system (53).
[b] T, primary tumor; N, regional lymph nodes; M, distant metastasis.

Immunohistochemistry and hematoxylin and eosin (HE) staining. Paraffin-embedded specimens were deparaffinized and rehydrated using dimethylbenzene, followed by serial ethanol washes. Antigen unmasking was performed by incubating each section in sodium citrate-hydrochloric acid buffer in a pressure cooker at 125°C for 10 to 15 min. The sections were washed in distilled water and then in Tris-buffered saline (TBS). The sections then were incubated in 5% goat serum–1% bovine serum albumin (BSA) in TBS for 1 h at room temperature, followed by staining with hematoxylin and washing with water. This was followed by two washes with water and two washes with 70% ethanol. The samples then were stained with eosin and dehydrated with ethanol followed by dimethylbenzene. For immunohistochemical staining, primary antibodies were used according to the manufacturer's instructions; the samples then were processed using the SP immunohistochemical kit (Maixin, Fuzhou, China), and the immunoreactive proteins were detected using a DAB kit according to the manufacturer's instructions (Maixin, Fuzhou, China).

Semiquantitative evaluation of immunohistochemical staining. The paraffin-embedded samples were cut into 5-μm sections and processed for immunohistochemical analysis. As a negative control, the primary antibody was replaced with normal murine or rabbit IgG. According to the method of Li et al. (22), MTA1 immunoreactivity was scored using a semiquantitative scoring system incorporating the proportion of positively stained tumor cells (0, ≤5%; 1, 6 to 25%; 2, 26 to 50%; 3, 51 to 75%; 4, ≥76%) and the intensity of staining (0, no staining; 1, light yellow weak staining; 2, yellow-brown moderate staining; 3, brown strong staining) to

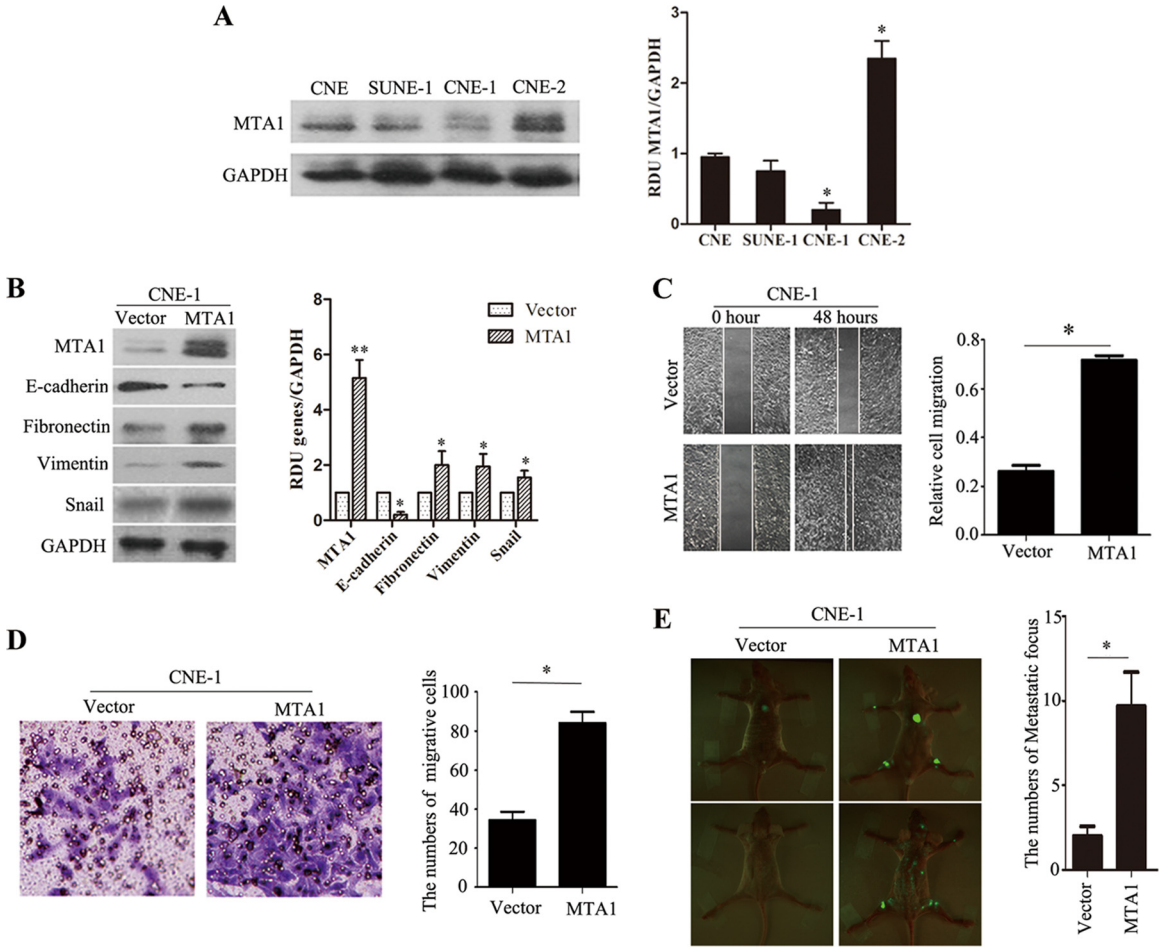

FIG 2 Overexpression of MTA1 induced EMT of CNE-1 cell lines both *in vitro* and *in vivo*. (A) The levels of the MTA1 protein in 4 NPC cell lines were examined by Western blotting. The blots are representative of two independent experiments. (Right) The histogram is the mean densitometric analysis showing relative density units (RDU) of the Western blot signal for MTA1 normalized to GAPDH. All data represent means ± standard errors of the means (SEM). *, $P < 0.05$ by Student's *t* test. (B) Western blot assays showed decreased levels of an epithelial marker (E-cadherin) and increased levels of mesenchymal markers (snail, fibronectin, and vimentin) in CNE-1-MTA1 cells compared to CNE-1-vector cells. The blots are representative of two independent experiments, and the quantification of independent experiments is shown on the right. All data represent means ± SEM. *, $P < 0.05$; **, $P < 0.01$ by Student's *t* test. (C) Wound-healing assays demonstrated that CNE-1-MTA1 cells had higher motility than CNE-1-vector cells. The numbers of migrating cells in the CNE-1-vector and CNE-1-MTA1 groups are shown on the right ($n = 2$ per condition). All data represent means ± SEM. *, $P < 0.05$ by Student's *t* test. (D) The ectopic overexpression of MTA1 enhanced CNE-1 cell invasion in a transwell assay. The purple color in the figure shows invaded cells ($n = 3$ per condition). All data represent means ± SEM. *, $P < 0.05$ by independent Student's *t* test. (E) The overexpression of MTA1 promoted CNE-1 cell invasion and metastasis in nude mice tumor models. Left, representative metastatic nodules (green spots) in nude mice; right, the number of metastatic nodules formed in nude mice 3 weeks after cell injection (4 mice per group). The error bars indicate means ± SEM. *, $P < 0.05$ by independent Student's *t* test.

result in a score of 0, 1, 2, 3, 4, 6, 8, 9, or 12 (data not shown). The cutoff values for high and low expression were selected on the basis of a measure of heterogeneity using the log-rank test statistical analysis with respect to overall survival. The optimal cutoff value was defined as 4; tumors with scores of ≤4 were defined as having low MTA1 expression, while tumors with scores of >4 had high MTA1 expression.

Western blotting. Whole cells were washed in PBS and lysed in radioimmunoprecipitation assay (RIPA) lysis buffer supplemented with protease inhibitor cocktail (Roche, Mannheim, Germany). Cytoplasmic and nuclear extracts were obtained using NE-PER nuclear and cytoplasmic extraction reagents (Thermo Scientific Pierce, Thermo Fisher Scientific, Rockford, IL, USA). Total protein was quantified using a bicinchoninic acid (BCA) protein assay kit (Beyotime, Jiangsu, China), and an equal amount of whole-cell lysates was resolved by SDS-PAGE and transferred to a polyvinylidene difluoride (PVDF) membrane (Millipore, Eschborn, Germany). The blots were blocked in BSA (5%, wt/vol, in PBS plus 0.1% Tween 20) for 1 h at room temperature. The following primary antibodies were used according to the manufacturer's instructions. Antibodies against LMP2A, MTA1, snail, vimentin, β-actin, and glyceraldehyde-3-phosphate dehydrogenase (GAPDH) were purchased from Santa Cruz Biotechnology (Santa Cruz, CA). Antibodies against p-GSK3β^{S9}, glycogen synthase kinase 3β (GSK3β), Wnt1, p-mTOR^{S2448}, mTOR, p-Akt^{T308}, p-Akt^{S473}, Akt, p-p70S6K^{T389}, p70S6K, p-4EBP1$^{T37/46}$, p-rpS6$^{S240/244}$, rpS6, 4EBP1, eIF4E, c-myc, fibronectin, E-cadherin, histone H3, and β-catenin were purchased from Abcam (Cambridge, MA, USA). The appropriate secondary antibodies (Santa Cruz Biotechnology, Santa Cruz, CA, USA) were used at 1:1,000 (vol/vol) to 1:2,000 (vol/vol) dilutions in PBS plus 0.1% Tween 20 for 1 h at room temperature, and the signals were revealed using an ECL kit (Thermo Scientific Pierce, Thermo Fisher Scientific, Rockford, IL, USA). INK-128 was purchased from Haoyuan Chemexpress Co. Ltd. (Shanghai, China). PF-4708671 was from Sigma (St. Louis, MO, USA).

Wound-healing and cell invasion assays. NPC cells were plated in 6-well plates and grown to confluence. The medium was removed, and

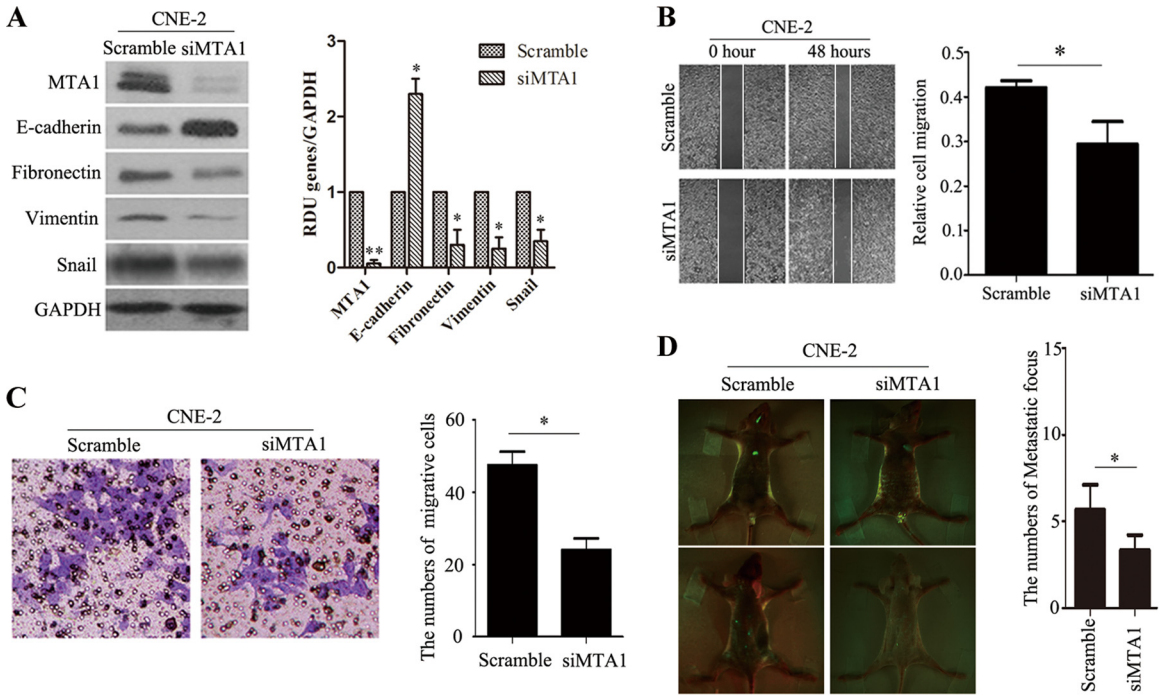

FIG 3 Silencing of MTA1 suppressed EMT of CNE-2 cell lines both *in vitro* and *in vivo*. (A) Western blot assays showed increased levels of an epithelial marker (E-cadherin) and decreased levels of mesenchymal markers (snail, fibronectin, and vimentin) in CNE-2-siMTA1 cells compared to CNE-2-scramble cells. The blots are representative of two independent experiments, and quantification of independent experiments is on the right. All data represent means ± SEM. *, $P < 0.05$; **, $P < 0.01$ by Student's *t* test. (B) Wound-healing assays showed that the motility of MTA1-silenced CNE-2 cells was lower than that of control cells ($n = 2$ per condition). All data represent means ± SEM. *, $P < 0.05$ by Student's *t* test. (C) The silence of MTA1 decreased CNE-2 cell-invasive capacity. The numbers of invading cells in the siMTA1 and scramble groups are shown on the right ($n = 3$ per condition). All data represent means ± SEM. *, $P < 0.05$ by independent Student's *t* test. (D) The silence of MTA1 decreased CNE-2 cell metastasis in nude mouse tumor models. Left, representative metastatic nodules (green spots) in nude mice; right, the number of metastatic nodules formed in nude mice 3 weeks after cell injection (4 mice per group). The error bars indicate means ± SEM. *, $P < 0.05$ by independent Student's *t* test.

wounds were introduced by scraping the confluent cell cultures with a 200-μl pipette tip. Floating cells were carefully removed before the addition of complete medium. The cells were incubated at 37°C in a humidified atmosphere of 95% air and 5% CO_2. The wound-healing process then was monitored by inverted light microscopy (Zeiss, Germany). Transwell cell invasion assays were performed with BioCoat Matrigel (BD Biosciences, San Jose, CA) and invasion chambers (Millipore, Eschborn, Germany) with an 8-μm pore size according to the manufacturer's instructions. The cells were stained with crystal violet. A set of images was acquired using NIS Elements image analysis software (Nikon, Tokyo, Japan).

Dual-luciferase reporter assay. The MTA1 promoter sequence was cloned into the plasmid pGL3-Basic. Dual-luciferase assays (Promega, Madison, WI) were performed 36 h after transfection according to the manufacturer's protocol and detected with a Fluoroskan microplate reader (Thermo Labsystems, Helsinki, Finland). The treated cells were lysed, and luciferase and renilla activities were analyzed using a dual-luciferase assay kit according to the manufacturer's instructions.

Immunofluorescence staining. Cells were grown in 20-mm-diameter glass-bottom culture plates to 60% confluence. The cells then were washed twice with PBS, fixed in 4% paraformaldehyde, permeabilized in 0.5% Triton X-100 in PBS for 10 min at 4°C, and processed for immunofluorescence staining. All primary antibody incubations were performed overnight at 4°C, and the primary antibodies were used at the following dilutions: anti-MTA1, 1:200; anti-β-catenin, 1:200. Secondary antibodies were Alexa Fluor 488 goat anti-mouse IgG, Alexa Fluor 647 goat anti-mouse IgG, and Alexa Fluor 488 goat anti-rabbit IgG (Abcam, Cambridge, MA). Finally, the cells were washed, mounted with mounting medium containing 4′,6-diamidino-2-phenylindole (DAPI; Santa Cruz Biotechnology, Santa Cruz, CA), and imaged using an Olympus FV1000 confocal microscope (Olympus, Lake Success, NY).

***In vivo* metastasis model.** Nude mice were purchased from Vital River Laboratories (Beijing, China) and maintained in microisolator cages. All animals were used in accordance with institutional guidelines, and the experiments were approved by the Use Committee for Animal Care. All cultures used for injection were subconfluent and were fed the day prior to use. The harvested cell suspension was washed twice by centrifugation in medium containing serum at room temperature and then resuspended in medium without serum at 4°C immediately prior to injection. The number of cells to be injected was suspended in 0.1 ml PBS. For intravenous injection of tumor cells, 6-week-old BALB/c nude mice were warmed 10 min away from a 150-W light bulb for 20 to 30 min. The cells were injected into a lateral tail vein. The animals were sacrificed 3 weeks after injection. For intracardiac injection into the left ventricle using a Stereotaxic instrument, 6-week-old BALB/c nude mice were anesthetized by injection of ketamine. The animals were sacrificed 3 weeks after injection. The viscera were removed, and the viscera and carcass were fixed in 10% formalin for subsequent HE staining and immunohistochemical analysis. Macro imaging was performed using UV light equipment (LT-99D2-220 Illumatools; Lightools Research, Encinitas, CA). Pictures were recorded with a Nikon d800 digital camera (Nikon, Tokyo, Japan). Images were processed for contrast and brightness and analyzed by Image Pro Plus 5.1 software (Media Cybernetics, Silver Spring, MD). The green signals or spots represent GFP-labeled cells.

Statistical analysis. The expression of MTA1 in the tissue samples was evaluated using chi-square tests. GraphPad Prism, version 4.0 (GraphPad Software, San Diego, CA, USA), was used to obtain the histogram. Statis-

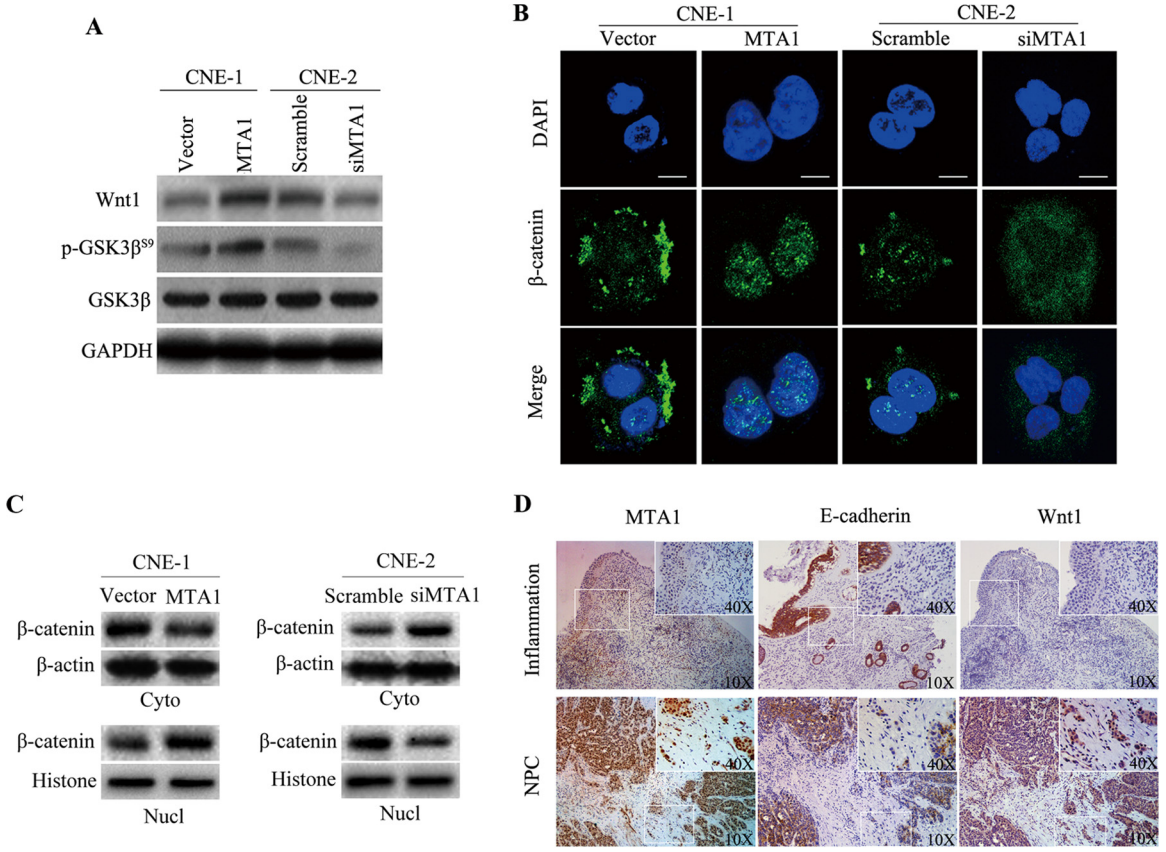

FIG 4 MTA1 mediates EMT, migration, and invasion by enhancing the expression of biologically active Wnt1 in NPC cell lines. (A) Representative Western blot from three independent experiments of CNE-1-vector, CNE-1-MTA1, CNE-2-scramble, and CNE-2-siMTA1 cells for the expression of Wnt1 and GSK3β phosphorylation analysis. The quantification of the Western blot signals are analyzed (data not shown). (B) Confocal image of β-catenin (green) expression in CNE-1-vector, CNE-1-MTA1, CNE-2-scramble, and CNE-2-siMTA1 cells. The scale bar depicts 10 μm. (C) CNE-1-vector, CNE-1-MTA1, CNE-2-scramble, and CNE-2-siMTA1 cells were subjected to nuclear (Nucl) and cytoplasmic (Cyto) extract isolation. The blots are representative of two independent experiments. The quantification of the Western blot signal for β-catenin was normalized to either β-actin or histone compared to untreated controls (data not shown). (D) The expression of MTA1, E-cadherin, and Wnt1 was determined by immunohistochemical analysis in inflammatory or NPC tumor biopsy specimens. The insets show images at a higher magnification. Positive staining is visible as brown spots.

tical analyses were performed using SPSS, v. 11.0 (SPSS, Inc., Chicago, IL). A P value of <0.05 was considered statistically significant.

RESULTS

Immunohistochemical staining of MTA1 expression in nasopharyngeal carcinoma tissues and its correlation with the clinicopathological features of NPC patients. To investigate the expression of MTA1 in NPC, we performed immunohistochemical staining of MTA1 in an NPC specimen bank containing 60 NPC specimens and 10 nasopharyngeal inflammation tissues. The immunohistochemical staining of MTA1 in representative samples of NPC and nasopharyngeal inflammation tissues is shown in Fig. 1B. Semiquantitative evaluation of immunohistochemical staining criterion was used to classify high and low expression of MTA1 for Table 1. Correlation analysis demonstrated that the overexpression of MTA1 was positively correlated with NPC lymph node ($P < 0.01$) (Table 1), distant metastases ($P = 0.03$) (Table 1), and the expression of LMP2A ($P = 0.03$) (Table 1). However, this correlation was not significant between the overexpression of MTA1 and sex ($P = 0.46$) (Table 1), tumor size ($P = 0.13$) (Table 1), or tumor clinical stage ($P = 0.06$) (Table 1). There was no correlation of age with the expression of MTA1.

MTA1 expression correlates with the expression of EMT-like markers in NPC samples. Because the overexpression of MTA1 was positively correlated with tumor metastasis, we next examined the location of the overexpressed MTA1 in tumor tissues. As shown in Fig. 1A, the overexpressed MTA1 was detected mainly in the areas of overlap between normal tissues and tumor tissues, as well as in the areas of tumor squamous metaplasia and lymphonodus (data not shown), indicating an invasive role of MTA1 in tumor invasion. To determine if there was a correlation between MTA1 expression and representative markers of EMT in the NPC and inflammation biopsy samples, we analyzed and detected MTA1, vimentin (a marker of mesenchymal tissues), and E-cadherin (a marker of epithelial tissues) in NPC biopsy specimens or inflammation biopsy specimens. As shown in Fig. 1B and C, the expression of MTA1 was positively correlated with vimentin expression and negatively correlated with E-cadherin expression. These results indicate that MTA1 expression is correlated with the expression of EMT-like markers in NPC samples and plays a role in the EMT of NPC.

MTA1 expression levels influence the invasive capacity of NPC cell lines *in vitro* and *in vivo*. Of the 4 NPC cell lines ana-

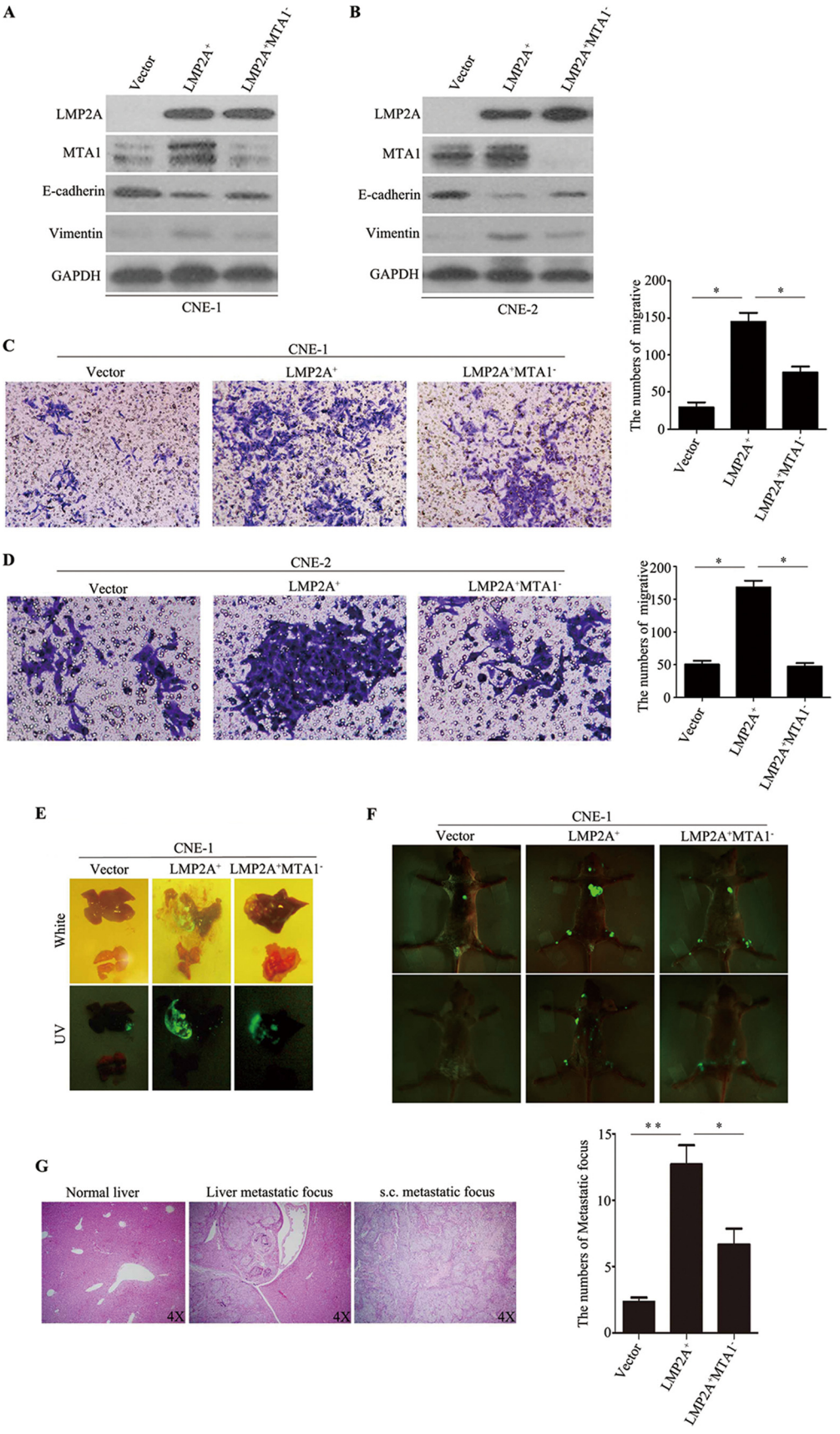
A
Vector
LMP2A+
LMP2A+MTA1-
LMP2A
MTA1
E-cadherin
Vimentin
GAPDH
CNE-1
B
Vector
LMP2A+
LMP2A+MTA1-
LMP2A
MTA1
E-cadherin
Vimentin
GAPDH
CNE-2
C
CNE-1
Vector
LMP2A+
LMP2A+MTA1-
The numbers of migrative
200
150
100
50
0
*
*
Vector
LMP2A+
LMP2A+MTA1-
D
CNE-2
Vector
LMP2A+
LMP2A+MTA1-
The numbers of migrative
200
150
100
50
0
*
*
Vector
LMP2A+
LMP2A+MTA1-
E
CNE-1
Vector
LMP2A+
LMP2A+MTA1-
White
UV
F
CNE-1
Vector
LMP2A+
LMP2A+MTA1-
G
Normal liver
Liver metastatic focus
s.c. metastatic focus
4X
4X
4X
The numbers of Metastatic focus
15
10
5
0
**
*
Vector
LMP2A+
LMP2A+MTA1-

lyzed by Western blotting, endogenous high MTA1 expression was detected only in CNE-2 cells, whereas the other 3 lines (i.e., CNE, CNE-1, and SUNE-1) displayed low levels of endogenous MTA1 expression (Fig. 2A). CNE-1 cells then were used to study the role of MTA1 in tumor invasion. To determine if overexpression of MTA1 could enhance the invasive capacity of NPC cells, we constructed the cell line CNE-1-MTA1, which overexpresses MTA1 (Fig. 2B). Western blotting revealed that the overexpression of MTA1 resulted in decreased expression of epithelial markers (E-cadherin) and increased expression of mesenchymal markers (fibronectin and vimentin) in CNE-1-MTA1 cells compared to cells containing the control vector; these results are consistent with our previous patient sample data. In addition, Snail expression was increased in CNE-1-MTA1 cells compared to that in the control. The wound-healing assay demonstrated that the overexpression of MTA1 enhanced CNE-1 cell migration at the edge of the exposed regions (Fig. 2C). A Matrigel invasion assay revealed that the invasive capacity of CNE-1-MTA1 cells was significantly greater than that of the control CNE-1-vector cells (Fig. 2D). Taken together, these results confirmed that MTA1 has significant effects on the invasive capacity of the low MTA1-expressing NPC cell line, CNE-1.

Because immunohistochemical analysis indicated that MTA1 overexpression was positively associated with NPC metastasis, we next used a high MTA1-expressing cell line, CNE-2, to determine if lentivirus-mediated MTA1 silencing decreased the tumor invasiveness of NPC cells. Specific siRNA targeting MTA1 efficiently knocked down endogenous MTA1 in CNE-2 (Fig. 3A). MTA1 knockdown resulted in the increased expression of E-cadherin and decreased expression of fibronectin, vimentin, and Snail in CNE-2 cells *in vitro* compared to the control scramble-treated cells. The wound-healing assay indicated that MTA1 knockdown caused an apparent suppression of cell migration by CNE-2 cells (Fig. 3B). Matrigel invasion assays also demonstrated that the ablation of endogenous MTA1 markedly reduced the invasive ability of CNE-2 cells (Fig. 3C). Collectively, these results provide evidence that elevated MTA1 expression levels are important for the aggressive phenotype of NPC cells.

To determine if MTA1 expression levels are correlated with metastasis in an experimental metastasis model, we injected CNE-1-MTA1 and CNE-2-siMTA1 cells into the left ventricle of nude mice; the CNE-1-vector and CNE-2-scramble cells were used as controls (each group consisted of 4 mice). Three weeks after cell injection, the mice were sacrificed and the metastatic tumor nodules that formed in the muscle and skeleton were examined. More metastatic tumor nodules were observed in the muscles and skeletons of mice that were injected with CNE-1-MTA1 cells compared to CNE-1-vector control mice (Fig. 2E), and fewer metastatic tumor nodules (green spots) were observed in the muscles and skeletons of mice injected with CNE-2-siMTA1 cells (Fig. 3D) compared to those injected with the CNE-2-scramble control. These results indicate that MTA1 is a critical tumor invasive factor *in vitro* and *in vivo*.

MTA1-Wnt and the Wnt1-GSK3β axis mediate β-catenin activation. The expression of Wnt1 is upregulated in various cancers (37, 38). Metastatic tumor antigen (MTA1) recently was shown to stimulate the expression of bioactive Wnt1 (33, 39). We hypothesized that MTA1 plays a role in the induction of Wnt1 upregulation in NPC cells; therefore, it increases tumor metastasis. We examined the effects of both the silencing and overexpression of MTA1 in NPC cell lines. As we expected, in CNE-1 and CNE-2 cells, the overexpression of MTA1 enhanced Wnt1 protein levels, while the knockdown of MTA1 decreased Wnt1 protein levels (Fig. 4A). We then investigated whether the effects of MTA1 on Wnt1 would affect the levels of the downstream Wnt1 signaling pathway molecules β-catenin and GSK3β. GSK3β is catalytically active in resting cells. GSK3β enzymatic activity is inhibited by phosphorylation and leads to the modulation of downstream targets. As shown in Fig. 4A, the overexpression of MTA1 resulted in increased GSK3β phosphorylation. Another important molecule, β-catenin, translocated from the cytoplasm into the nucleus via Western blotting and immunofluorescence analysis when MTA1 was overexpressed and remained in the cytoplasm when MTA1 was knocked down (Fig. 4B and C). In addition, we also detected the MTA1, E-cadherin, and Wnt1 proteins in NPC and inflammation biopsy specimens (Fig. 4D); immunohistochemical staining demonstrated that NPC biopsy specimens exhibit decreased expression of E-cadherin and increased expression of Wnt1 compared to inflammation biopsy specimens. These data reveal that the overexpression of MTA1 increases NPC cell invasive capacity by activating the Wnt1 signaling pathway.

LMP2A induces EMT in part by enhancing the expression levels of MTA1. Because LMP2A induces EMT and stem-like cell self-renewal in NPC, it was important to examine whether MTA1 plays a role in the LMP2A-induced EMT in NPC cells. CNE-1 and CNE-2 cells were infected with lentivirus expressing either lentivirus-LMP2A or an empty vector. LMP2A protein overexpression was detectable by immunoblotting. As shown in Fig. 5A and B, MTA1 protein expression was increased in CNE-1-LMP2A and CNE-2-LMP2A cell lines in which LMP2A is ectopically overexpressed. To determine if LMP2A induces EMT via the activation of MTA1, we constructed the cell lines CNE-1-LMP2A$^+$MTA1$^-$ and CNE-2-LMP2A$^+$MTA1$^-$, which express LMP2A but have minimal MTA1 protein expression. Western blotting revealed that the knockdown of MTA1 resulted in the increased expression of an epithelial marker (E-cadherin) and decreased expression of a

FIG 5 LMP2A mediates EMT, migration, and invasion of NPC cells partly by activating MTA1 expression. (A and B) Western blot assay showing that LMP2A activated MTA1 expression in both CNE-1-LMP2A and CNE-2-LMP2A cells, decreased levels of an epithelial marker (E-cadherin), and increased levels of mesenchymal markers (vimentin) in CNE-1-LMP2A$^+$MTA1$^-$ cells compared to CNE-1-LMP2A cells and CNE-2 cells. The blots are representative of two independent experiments. The quantification of the Western blot signals was analyzed (data not shown). (C and D) The silencing of MTA1 decreased the invasive capacity of CNE-1-LMP2A and CNE-2-LMP2A cells. The number of invading cells in the siMTA1 and scramble groups is shown on the right ($n = 2$ per condition). All data represent means ± SEM.*, $P < 0.05$ by independent Student's *t* test. (E) Representative metastatic nodules formed in the liver of nude mice 4 weeks after liver injection of cells (four mice per group). (F) The expression of LMP2A promoted CNE-1 cell invasion and metastasis, and the silencing of MTA1 decreased CNE-1-LMP2A cell invasion and metastasis in nude mice. Upper images, representative metastatic nodules (green spots) in nude mice; lower images, the number of metastatic nodules formed in nude mice 3 weeks after cell injection (4 mice per group). The error bars indicate means ± SEM. *, $P < 0.05$; **, $P < 0.01$ by independent Student's *t* test. (G) Examples of HE staining in subcutaneous (s.c.) and liver nodule samples originating from CNE-1-vector cell- and CNE-1-LMP2A cell-injected mice.

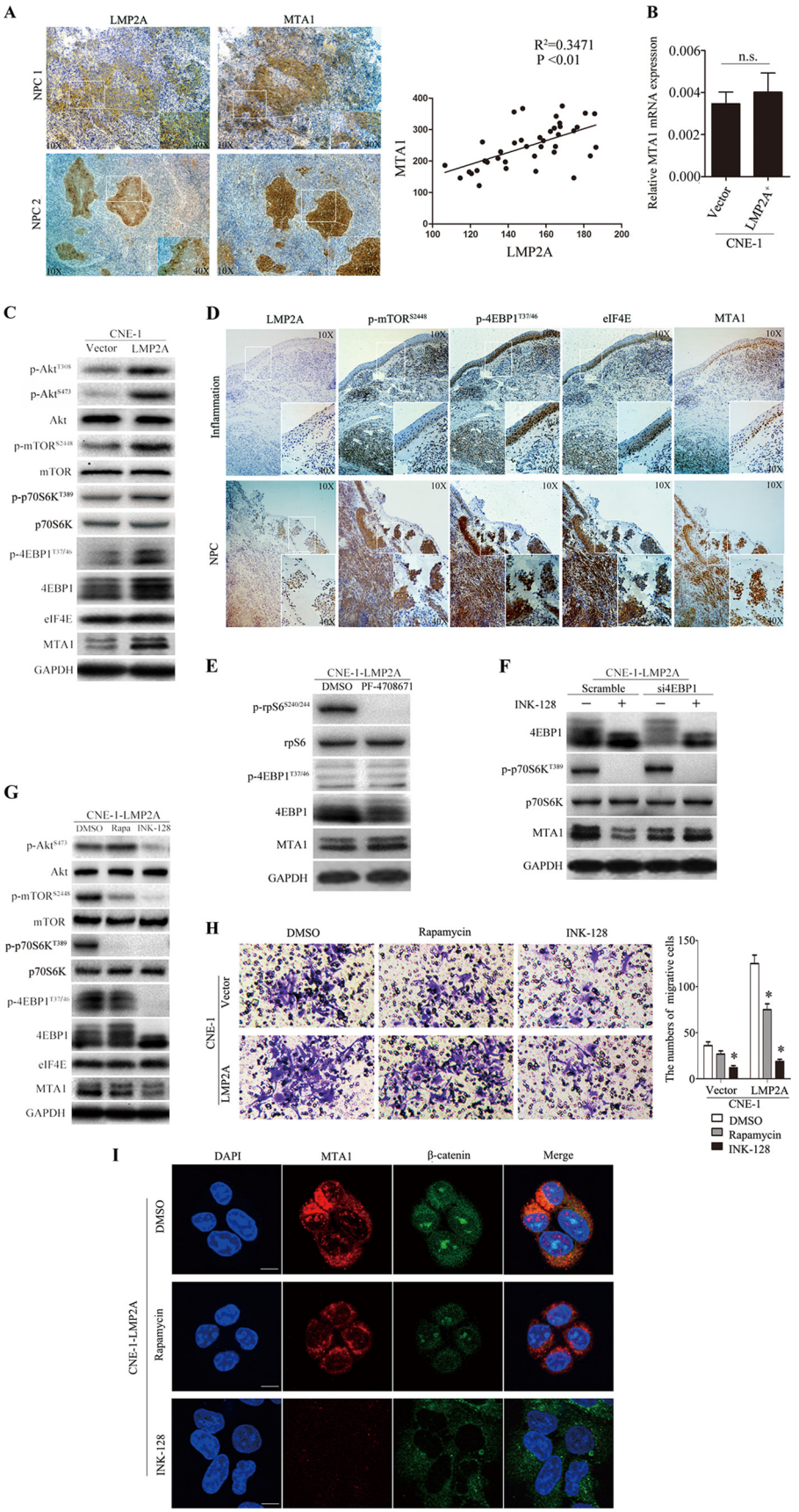
A
LMP2A
MTA1
NPC 1
NPC 2
10X
40X
R²=0.3471
P <0.01
MTA1
LMP2A
B
Relative MTA1 mRNA expression
n.s.
Vector
LMP2A
CNE-1
C
CNE-1
Vector
LMP2A
p-AktT308
p-AktS473
Akt
p-mTORS2448
mTOR
p-p70S6KT389
p70S6K
p-4EBP1T37/46
4EBP1
eIF4E
MTA1
GAPDH
D
LMP2A
p-mTORS2448
p-4EBP1T37/46
eIF4E
MTA1
Inflammation
NPC
E
CNE-1-LMP2A
DMSO
PF-4708671
p-rpS6S240/244
rpS6
p-4EBP1T37/46
4EBP1
MTA1
GAPDH
F
CNE-1-LMP2A
Scramble
si4EBP1
INK-128
4EBP1
p-p70S6KT389
p70S6K
MTA1
GAPDH
G
CNE-1-LMP2A
DMSO
Rapa
INK-128
p-AktS473
Akt
p-mTORS2448
mTOR
p-p70S6KT389
p70S6K
p-4EBP1T37/46
4EBP1
eIF4E
MTA1
GAPDH
H
DMSO
Rapamycin
INK-128
CNE-1
Vector
LMP2A
The numbers of migrative cells
Vector
LMP2A
CNE-1
DMSO
Rapamycin
INK-128
I
DAPI
MTA1
β-catenin
Merge
CNE-1-LMP2A
DMSO
Rapamycin
INK-128

mesenchymal marker (vimentin) in these cells compared to the levels in control cells (Fig. 5A and B). Wound-healing assays demonstrated that MTA1 knockdown decreased CNE-1-LMP2A and CNE-2-LMP2A cell migration at the edges of the exposed regions (data not shown). The Matrigel invasion assay also revealed that the invasive capacities of CNE-1-LMP2A$^+$MTA1$^-$ and CNE-2-LMP2A$^+$MTA1$^-$ cells were significantly decreased compared to those of our control cells (Fig. 5C and D). We then investigated invasive capacity in the mouse model. Because the CNE-1 cell line has a low level of endogenous MTA1 expression, the nude mice were infused with CNE-1-LMP2A, CNE-1-LMP2A$^+$MTA1$^-$, and control cells into the liver and left ventricle. As shown in Fig. 5E and F, CNE-1-LMP2A$^+$MTA1$^-$ cells formed more tumor lesions (green spots) in the liver, muscle, and skeleton. HE staining of tumor lesions is shown in Fig. 5G. The *in vivo* data are consistent with the *in vitro* data, which suggested that LMP2A induces EMT and enhances NPC invasive capacity in part via the MTA1 signaling pathway.

LMP2A induces the expression of MTA1 through the activation of mTOR signaling pathway. As described above, LMP2A mediates transformation via the constitutive activation of the Ras/PI3K/Akt pathway (40). mTOR is a downstream serine/threonine kinase of the PI3K/Akt pathway that integrates signals from the tumor microenvironment to regulate multiple cellular processes. The translational control of MTA1 mRNA recently was found to rely on the 4EBP1-eIF4E axis (34). To investigate the correlation between LMP2A and MTA1 in NPC, we performed correlation analysis of LMP2A and MTA1 by intensity optical density (IOD) means of immunohistochemical staining in NPC specimens and demonstrated that the expression of LMP2A was positively correlated with MTA1 overexpression (Fig. 6A). To address whether LMP2A induces the expression of MTA1 through mTOR activation, we used CNE-1-LMP2A cells to study these signaling pathways, as CNE-1 cells have low levels of endogenous MTA1. First, we examined the transcription level of MTA1 mRNA in CNE-1-LMP2A and control cells, but there was no significant difference between them (Fig. 6B). This result led us to focus on the translational regulatory mechanism of mTOR in this study. As shown in Fig. 6C, overexpression of LMP2A resulted in increased expression of p-Akt, p-mTOR, p-p70S6K, p-4EBP1, and MTA1. LMP2A, p-mTOR, p-4EBP1, eIF4E, and MTA1 protein expression also was assessed in NPC and inflammation biopsy specimens. Immunohistochemical staining demonstrated that the tissues from NPC biopsy specimens had increased levels of p-mTOR, p-4EBP1, eIF4E, and MTA1 expression compared to the tissues from the inflammation biopsy specimens (Fig. 6D). These data indicated that LMP2A induction of MTA1 expression occurs through the 4EBP1-eIF4E axis.

We then studied whether 4EBP1 and/or p70S6K, which are the translational regulators downstream of mTORC1, control the expression of MTA1. As shown in Fig. 6E, the pharmacological PF-4708671, a novel and highly specific inhibitor of p70 ribosomal S6 kinase (41), had no effect on MTA1 expression, while knockdown of 4EBP1 in CNE-1-LMP2A cells reduced the ability of INK128 to decrease expression of MTA1 (Fig. 6F). INK-128, a potent and selective mTOR inhibitor, inhibits the mTOR pathway by inhibiting p-4EBP1, whereas rapamycin fails to inhibit this downstream protein (6). We used INK-128 to inhibit p-4EBP1 in the CNE-1-LMP2A cells to further test our findings. E-cadherin expression was increased, and the levels of expression of a mesenchymal marker (vimentin), Wnt1, and Snail were decreased in CNE-1-LMP2A cells 48 h after INK-128 treatment compared to control dimethylsulfoxide (DMSO)-treated cells (data not shown). In addition, levels of p-AKT, p-mTOR, p-p70S6K, p-4EBP1, eIF4E, c-myc, and MTA1 all were decreased in INK-128-treated CNE-1-LMP2A cells compared to those of control DMSO- and rapamycin-treated cells (Fig. 6G). Wound-healing assays demonstrated that treatment with INK-128 decreased CNE-1-LMP2A cell migration at the edge of the exposed regions compared to treatment with DMSO or rapamycin (data not shown). The Matrigel invasion assay also showed that the invasive capacity of INK-128-treated CNE-1-LMP2A cells was significantly decreased compared to that of control cells (Fig. 6H). Western blotting and immunofluorescence analysis of MTA1 and β-catenin expression revealed that MTA1 was decreased and β-catenin was maintained in the cytoplasm when the cells were treated with INK-128 (Fig. 6I and data not shown).

The 4EBP1-eIF4E axis directly increases the expression of the MTA1 protein by posttranslational regulation, but it also may increase the level of c-myc protein expression. Because MTA1 is an essential downstream effector of the c-myc oncoprotein (31), we next addressed whether LMP2A induces the expression of MTA1 partly or entirely through c-myc. We examined LMP2A and c-myc protein expression in NPC and inflammation biopsy specimens (Fig. 7A). Western blotting revealed that c-myc expression was higher in CNE-1-LMP2A cells than in CNE-1-vector cells (Fig. 7B). Immunohistochemical staining demonstrated that c-myc expression was increased in the LMP2A-positive NPC biopsy specimens compared to the level in the inflammation biopsy specimens. To investigate the impact of c-myc on NPC cell invasiveness, we treated CNE-1-LMP2A cells with siRNA against c-myc. This siRNA could efficiently knock down endogenous c-myc

FIG 6 LMP2A induces an EMT, which occurs in part via the activation of MTA1 through the 4EBP1-eIF4E axis. (A) The expression of LMP2A and MTA1 NPC tumor biopsy specimens is determined by immunohistochemical analysis. The inset shows images at a higher magnification. The coordinate axis equals the IOD mean. (B) Representative real-time PCR from three independent experiments of CNE-1-LMP2A and CNE-1 cells for the expression of MTA1. All data represent means ± SEM. n.s., no difference. (C) Representative Western blot from three independent experiments of p-Akt, Akt, p-mTOR, mTOR, p-4EBP1, 4EBP1, eIF4E, c-myc, and MTA1 genes in CNE-1-LMP2A and vector control cells. The quantification of the Western blot signals are analyzed (data not shown). (D) Immunohistochemical analysis of LMP2A, p-mTOR, p-4EBP1, eIF4E, and MTA1 gene expression in inflammatory or NPC tumor biopsy specimens. The inset shows a higher-magnification image. (E) Representative Western blot from two independent experiments of CNE-1-LMP2A cells after 48 h PF-4708671 (10 μM) treatment. The quantification of the Western blot signals was analyzed (data not shown). (F) Representative Western blot from four independent experiments of CNE-1-LMP2A cells after 48 h of 4EBP1 knockdown followed by 24 h INK-128 treatment. The quantification of the Western blot signals was analyzed (data not shown). (G) Representative Western blot from two independent experiments of p-Akt, p-mTOR, mTOR, p-4EBP1, 4EBP1, eIF4E, c-myc, and MTA1 genes in CNE-1-LMP2A cells treated with rapamycin (50 nM) or INK-128 (200 nM) for 24 h. The quantification of the Western blot signals are analyzed (data not shown). (H) Matrigel cell invasion assay of CNE-1-LMP2A cells treated with rapamycin (50 nM) or INK-128 (200 nM) for 24 h. The numbers of invading cells are shown on the right ($n = 3$ per condition). All data represent means ± SEM. *, $P < 0.05$ by independent Student's t test. (I) Confocal analysis of MTA1 (red) and β-catenin (green) expression in CNE-1-LMP2A cells treated with rapamycin (50 nM) or INK-128 (200 nM) for 24 h. The scale bar represents 10 μm.

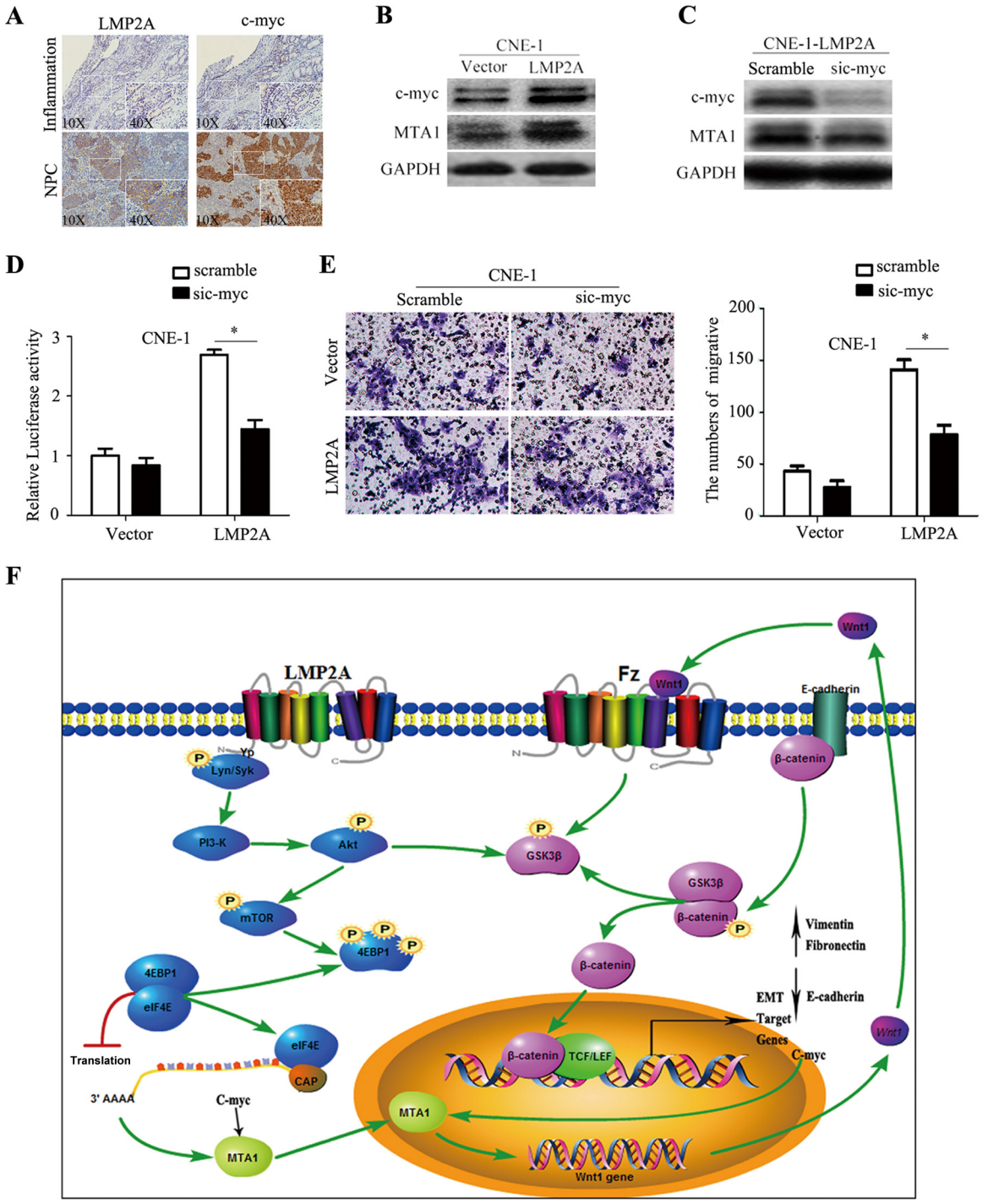

FIG 7 LMP2A-mediated EMT, migration, and invasion in NPC cell lines are partly inhibited by the silencing of c-myc. (A) Immunohistochemical analysis of LMP2A and c-myc expression in inflammation or NPC tumor biopsy specimens. Positive staining is visible as brown spots. The inset shows a higher-magnification image. (B) Representative Western blot from two independent experiments of c-myc and MTA1 genes in CNE-1-LMP2A and vector control cells. The quantification of the Western blot signals was analyzed (data not shown). (C) Representative Western blot from two independent experiments of c-myc and MTA1 gene expression after knockdown of c-myc using a specific siRNA. The quantification of the Western blot signals was analyzed (data not shown). (D) Luciferase assay analysis of the MTA1 promoter. CNE-1 and CNE-1-LMP2A cells first were transfected with sic-myc or scramble siRNA. After 36 h, the cells were cotransfected with the pGL3-MTA1 promoter luciferase and the pRL-TK renilla luciferase plasmid. The luciferase activity of the MTA1 promoter was measured 36 h later and normalized relative to luciferase activity. The bar shows the means ± SEM from 3 independent experiments. *, $P < 0.05$ by Student's *t* test. (E) The silencing of c-myc decreased CNE-1-LMP2A cell invasive capacity. The numbers of invading cells in the sic-myc and scramble groups are shown on the right ($n = 2$ per condition). All data represent means ± SEM. *, $P < 0.05$ by independent Student's *t* test. (F) Schematic model of LMP2A promotes EMT in NPC via MTA1 and mTOR signal induction. LMP2A ITAMs (immunoreceptor tyrosine-based activation motifs) activate PI3K and downstream phosphorylation of Akt and then stimulate mTOR activity. The phosphorylation of 4EBP1 by mTOR releases eIF4E to restore cap-dependent translation, which is particularly important for the translation of MTA1 and c-myc mRNA. LMP2A stimulates MTA1 overexpression, leading to decreased E-cadherin expression that releases β-catenin and increased Wnt1 expression that phosphorylates GSK3β. Unphosphorylated GSK3β forms a destruction complex as well as ubiquitination and degradation of β-catenin, resulting in repression of target genes. LMP2A stimulation leads to phosphorylation of GSK3β, rendering it inactive, which leads to the disintegration of the destruction complex. These events lead to accumulation and nuclear translocation of β-catenin as well as activation of target genes.

in CNE-1-LMP2A cells (Fig. 7C). Furthermore, a dual-luciferase reporter assay showed that knocking down c-myc using this specific siRNA only partly inhibited the transcriptional activity of MTA1 (Fig. 7D). Matrigel invasion assays also demonstrated that the ablation of endogenous c-myc partly reduced the invasive ability of CNE-1-LMP2A cells (Fig. 7E). Hence, these data suggested that LMP2A could induce EMT by activating MTA1 at the translational level through the 4EBP1-eIF4E axis and partially through c-myc regulation (Fig. 7F).

DISCUSSION

MTA1 plays a key role in the nucleosome remodeling and histone deacetylase (NuRD) complex. It governs oncogenesis and EMT in a transcription-dependent or transcription-independent manner (42). Dysregulated MTA1 promotes EMT, which mediates the repression of E-cadherin and PTEN expression (30, 43). In our study, the expression level of MTA1 predicts the rate of tumor metastasis. Specific staining of MTA1 was found in the squamous metaplasia, breakthrough basement membrane, and squamous metaplasia (Fig. 1A and data not shown). We believe that MTA1 is also a very important regulator of NPC invasiveness both *in vitro* and *in vivo*. It is reported that MTA1 also affects the hypoxia-inducible factor 1a and Wnt1 pathways (44, 45), which also have been implicated in EMTs through multiple distinct mechanisms. Immunohistochemical analysis showing MTA1 overexpression leads to decreased E-cadherin expression and increased Wnt1 expression (Fig. 4D and data not shown). Furthermore, we also demonstrated that MTA1 involved in the Wnt1-β-catenin pathway was correlated with EMT in NPC. It strongly indicated MTA1 overexpression is responsible for the invasive capacity of NPC. These events lead to accumulation, nuclear translocation of β-catenin, and activation of target genes. Since we already know that MTA1 participates in NPC invasiveness, it remains unknown which factors initiate MTA1 overexpression in NPC.

The EBV protein LMP2A mediates transformation via the constitutive activation of the Ras/PI3K/Akt pathway (46). Akt phosphorylation was detected both in cell and NPC tumor squamous metaplasia (Fig. 6C and data not shown). Hsieh et al. have suggested that YB1 (Y-box binding protein 1; also called YBX1), vimentin, MTA1, and CD44, which form the second largest node of genes that are translationally regulated by mTOR, contains *bona fide* cell invasion and metastasis mRNAs and putative regulators of this process (34). mTOR is a downstream serine/threonine kinase of the PI3K/Akt pathway that integrates signals from the tumor microenvironment to regulate multiple cellular processes (14). A positive feedback loop involving c-myc and eIF4F (eIF4E, eIF4AI, and eIF4GI) links transcription and translation and might contribute to the effects of c-myc on cell proliferation and neoplastic growth (46). EBV LMP2A induces EMT in NPC cells (12). This induction occurs through the PI3K/Akt/mTOR signaling pathway (47). On the basis of these findings, we proposed mTOR is a molecular hub connecting LMP2A activation and MTA1-induced tumor malignancy.

These results show that the regulation of MTA1 likely is affected by the translation mechanism of mTOR. mTOR has been implicated in the regulation of cell migration and adhesion (48). A novel clinically relevant mTOR inhibitor, INK128, inhibits p-4EBP1, on which rapamycin has no effect (34). Phosphorylation of 4EBP1 releases eIF4E to restore cap-dependent translation, which is particularly important for the translation of mRNAs with highly structured 5′ untranslated regions (49). To this end, we investigated whether the translational regulation of MTA1 could be induced by 4EBP1 and/or p70S6K, which are located downstream of mTOR. We found that PF-4708671 treatment inhibited p70S6K but not the protein level of MTA1. However, knockdown of 4EBP1 could increase the expression of MTA1 protein and release the translational regulation of the mRNA of MTA1. Furthermore, by using INK-128, we proved that the LMP2A-induced EMT depends on the activation of mTOR and the 4EBP1-eIF4E axis. Therefore, in this study, we furthered this concept by demonstrating that LMP2A induces EMT by activating MTA1, at least partially through the 4EBP1-eIF4E axis. This finding completes the molecular chain between LMP2A and EMT, thereby explaining the relationship between LMP2A and NPC cell malignancy.

mTOR could enhance the translation of both c-myc and MTA1, and MTA1 is an essential downstream effector of the c-myc oncoprotein (31). Recent studies have demonstrated that the overexpression of EIF5A2 promotes colorectal carcinoma cell aggressiveness by upregulating MTA1 through c-myc to induce EMT (32). Bultema et al. have reported that LMP2A accelerates c-myc tumorigenesis (50). Moody et al. have reported LMP2A modulation of the cell growth through c-myc, confirming a transcription-independent elevation in c-myc protein level but not mRNA level, consistent with mTOR-enhanced translation (14). Thus, LMP2A may participate in EMT induction by activating MTA1 via c-myc. In that case, whether mTOR regulates MTA1 directly or indirectly by c-myc still is unknown. As shown in Fig. 7C, the expression of MTA1 protein was decreased in a small quantity after knockdown of c-myc. The data indicate that LMP2A regulates the expression of MTA1 indirectly by inducing c-myc. To confirm this hypothesis, luciferase assay analysis of the MTA1 promoter was performed. Consistent with the Western blot analysis, we observed that CNE-1-LMP2A cells displayed decreased luciferase activity after knockdown of c-myc. However, CNE-1-LMP2A cells displayed increased invasive capacity compared to control cells after knockdown of c-myc. To sum up, this evidence suggests that the transcriptional regulation of MTA1 mRNA by c-myc is limited. However, the translational regulation of mTOR could enhance the protein expression level of MTA1. Consequently, the expression and function of MTA1 has been weakened when c-myc was knocked down (Fig. 7). There is a mutually reinforcing correlation between c-myc and mTOR. Therefore, we furthered this concept by demonstrating that LMP2A could induce EMT by activating MTA1 at the translational level through the 4EBP1-eIF4E axis and partially through c-myc regulation.

The consequences of the activation of LMP2A might cause other intracellular molecular events. Some of these events might alter mTOR, MTA1, or even EMT directly or indirectly. In other words, many interacting pathways might compensate for or compromise the effects of intermediate molecules in the signaling pathway of NPC. In summary, this study connects LMP2A, an oncoprotein of EBV and a well-known NPC activator, to the final effects of EMT and tumor metastasis by elucidating the activation of the mTOR signaling pathway. These findings add a novel mechanism to the complicated molecular network underlying NPC.

Currently, two mTOR inhibitors have been approved for the treatment of cancer by the U.S. Food and Drug Administration (51). Lapatinib given in combination with INK-128 is a potential combinatorial treatment available in the clinical management of

HER2-positive patients (52). This study bridges the gap between an NPC-specific cell surface molecule and the final phenotype of the NPC cells and, most importantly, verifies LMP2A and mTOR as therapeutic targets in NPC treatment.

ACKNOWLEDGMENTS

This work was supported by grants from the National Natural Science Foundation (30901750 and 81272322 to Y.C., 81201528 to R.J., 81201880 to L.D., and 81072029 to B.S.), the National Basic Research Program of China (2012CB910800 to B.S.), the Natural Science Foundation of Jiangsu Province (BK2010532 to Y.C.), the China Postdoctoral Science Foundation funded project (20090461133 to Y.C.), the Jiangsu Planned Projects for Postdoctoral Research Funds (1001028B to Y.C.), the Jiangsu Province Laboratory of Pathogen Biology (11BYKF02 to Y.C.), the Jiangsu Science and Technology Innovation Program for Graduate Research Funds (CXLX13-54 to X.W.), and the Priority Academic Program Development of Jiangsu Higher Education Institutions.

We also thank Hua Sun (Baylor College of Medicine, TX, USA) for language revision.

We have no conflicts of interest to disclose.

REFERENCES

1. **Wei WI, Sham JST.** 2005. Nasopharyngeal carcinoma. Lancet **365:**2041–2054. http://dx.doi.org/10.1016/S0140-6736(05)66698-6.
2. **Chan A, Teo P, Ngan R, Leung T, Lau W, Zee B, Leung S, Cheung F, Yeo W, Yiu H.** 2002. Concurrent chemotherapy-radiotherapy compared with radiotherapy alone in locoregionally advanced nasopharyngeal carcinoma: progression-free survival analysis of a phase III randomized trial. J. Clin. Oncol. **20:**2038–2044. http://dx.doi.org/10.1200/JCO.2002.08.149.
3. **Wang J, Guo L-P, Chen L-Z, Zeng Y-X, Lu SH.** 2007. Identification of cancer stem cell–like side population cells in human nasopharyngeal carcinoma cell line. Cancer Res. **67:**3716–3724. http://dx.doi.org/10.1158/0008-5472.CAN-06-4343.
4. **Langendijk J, Leemans CR, Buter J, Berkhof J, Slotman B.** 2004. The additional value of chemotherapy to radiotherapy in locally advanced nasopharyngeal carcinoma: a meta-analysis of the published literature. J. Clin. Oncol. **22:**4604–4612. http://dx.doi.org/10.1200/JCO.2004.10.074.
5. **Chua DT, Sham JS, Au GK.** 2003. A phase II study of capecitabine in patients with recurrent and metastatic nasopharyngeal carcinoma pretreated with platinum-based chemotherapy. Oral Oncol. **39:**361–366. http://dx.doi.org/10.1016/S1368-8375(02)00120-3.
6. **Kang Y, Massagué J.** 2004. Epithelial-mesenchymal transitions: twist in development and metastasis. Cell **118:**277–279. http://dx.doi.org/10.1016/j.cell.2004.07.011.
7. **Grünert S, Jechlinger M, Beug H.** 2003. Diverse cellular and molecular mechanisms contribute to epithelial plasticity and metastasis. Nat. Rev. Mol. Cell Biol. **4:**657–665. http://dx.doi.org/10.1038/nrm1175.
8. **Tellez CS, Juri DE, Do K, Bernauer AM, Thomas CL, Damiani LA, Tessema M, Leng S, Belinsky SA.** 2011. EMT and stem cell-like properties associated with miR-205 and miR-200 epigenetic silencing are early manifestations during carcinogen-induced transformation of human lung epithelial cells. Cancer Res. **71:**3087–3097. http://dx.doi.org/10.1158/0008-5472.CAN-10-3035.
9. **Mani SA, Guo W, Liao M-J, Eaton EN, Ayyanan A, Zhou AY, Brooks M, Reinhard F, Zhang CC, Shipitsin M.** 2008. The epithelial-mesenchymal transition generates cells with properties of stem cells. Cell **133:**704–715. http://dx.doi.org/10.1016/j.cell.2008.03.027.
10. **Brooks L, Yao Q, Rickinson A, Young L.** 1992. Epstein-Barr virus latent gene transcription in nasopharyngeal carcinoma cells: coexpression of EBNA1, LMP1, and LMP2 transcripts. J. Virol. **66:**2689–2697.
11. **Pegtel DM, Subramanian A, Sheen T-S, Tsai C-H, Golub TR, Thorley-Lawson DA.** 2005. Epstein-Barr-virus-encoded LMP2A induces primary epithelial cell migration and invasion: possible role in nasopharyngeal carcinoma metastasis. J. Virol. **79:**15430–15442. http://dx.doi.org/10.1128/JVI.79.24.15430-15442.2005.
12. **Kong Q-L, Hu L-J, Cao J-Y, Huang Y-J, Xu L-H, Liang Y, Xiong D, Guan S, Guo B-H, Mai H-Q.** 2010. Epstein-Barr virus-encoded LMP2A induces an epithelial-mesenchymal transition and increases the number of side population stem-like cancer cells in nasopharyngeal carcinoma. PLoS Pathog. **6:**e1000940. http://dx.doi.org/10.1371/journal.ppat.1000940.
13. **Lu J, Lin W-H, Chen S-Y, Longnecker R, Tsai S-C, Chen C-L, Tsai C-H.** 2006. Syk tyrosine kinase mediates Epstein-Barr virus latent membrane protein 2A-induced cell migration in epithelial cells. J. Biol. Chem. **281:**8806–8814. http://dx.doi.org/10.1074/jbc.M507305200.
14. **Moody CA, Scott RS, Amirghahari N, Nathan C-A, Young LS, Dawson CW, Sixbey JW.** 2005. Modulation of the cell growth regulator mTOR by Epstein-Barr virus-encoded LMP2A. J. Virol. **79:**5499–5506. http://dx.doi.org/10.1128/JVI.79.9.5499-5506.2005.
15. **Shaw RJ, Cantley LC.** 2006. Ras, PI (3) K and mTOR signalling controls tumour cell growth. Nature **441:**424–430. http://dx.doi.org/10.1038/nature04869.
16. **O'Reilly KE, Rojo F, She Q-B, Solit D, Mills GB, Smith D, Lane H, Hofmann F, Hicklin DJ, Ludwig DL.** 2006. mTOR inhibition induces upstream receptor tyrosine kinase signaling and activates Akt. Cancer Res. **66:**1500–1508. http://dx.doi.org/10.1158/0008-5472.CAN-05-2925.
17. **Chiang GG, Abraham RT.** 2007. Targeting the mTOR signaling network in cancer. Trends Mol. Med. **13:**433–442. http://dx.doi.org/10.1016/j.molmed.2007.08.001.
18. **Seeliger H, Guba M, Kleespies A, Jauch K-W, Bruns CJ.** 2007. Role of mTOR in solid tumor systems: a therapeutical target against primary tumor growth, metastases, and angiogenesis. Cancer Metast. Rev. **26:**611–621. http://dx.doi.org/10.1007/s10555-007-9077-8.
19. **Fukuda M, Longnecker R.** 2004. Latent membrane protein 2A inhibits transforming growth factor-β1-induced apoptosis through the phosphatidylinositol 3-kinase/Akt pathway. J. Virol. **78:**1697–1705. http://dx.doi.org/10.1128/JVI.78.4.1697-1705.2004.
20. **Scholle F, Bendt KM, Raab-Traub N.** 2000. Epstein-Barr virus LMP2A transforms epithelial cells, inhibits cell differentiation, and activates Akt. J. Virol. **74:**10681–10689. http://dx.doi.org/10.1128/JVI.74.22.10681-10689.2000.
21. **Toh Y, Pencil SD, Nicolson GL.** 1994. A novel candidate metastasis-associated gene, mta1, differentially expressed in highly metastatic mammary adenocarcinoma cell lines. cDNA cloning, expression, and protein analyses. J. Biol. Chem. **269:**22958–22963.
22. **Li W-F, Liu N, Cui R-X, He Q-M, Chen M, Jiang N, Sun Y, Zeng J, Liu L-Z, Ma J.** 2012. Nuclear overexpression of metastasis-associated protein 1 correlates significantly with poor survival in nasopharyngeal carcinoma. J. Transl. Med. **10:**78. http://dx.doi.org/10.1186/1479-5876-10-78.
23. **Gururaj AE, Singh RR, Rayala SK, Holm C, den Hollander P, Zhang H, Balasenthil S, Talukder AH, Landberg G, Kumar R.** 2006. MTA1, a transcriptional activator of breast cancer amplified sequence 3. Proc. Natl. Acad. Sci. USA **103:**6670–6675. http://dx.doi.org/10.1073/pnas.0601989103.
24. **Hofer MD, Kuefer R, Varambally S, Li H, Ma J, Shapiro GI, Gschwend JE, Hautmann RE, Sanda MG, Giehl K.** 2004. The role of metastasis-associated protein 1 in prostate cancer progression. Cancer Res. **64:**825–829. http://dx.doi.org/10.1158/0008-5472.CAN-03-2755.
25. **Sasaki H, Moriyama S, Nakashima Y, Kobayashi Y, Yukiue H, Kaji M, Fukai I, Kiriyama M, Yamakawa Y, Fujii Y.** 2002. Expression of the MTA1 mRNA in advanced lung cancer. Lung Cancer **35:**149–154. http://dx.doi.org/10.1016/S0169-5002(01)00329-4.
26. **Toh Y, Ohga T, Endo K, Adachi E, Kusumoto H, Haraguchi M, Okamura T, Nicolson GL.** 2004. Expression of the metastasis-associated MTA1 protein and its relationship to deacetylation of the histone H4 in esophageal squamous cell carcinomas. Int. J. Cancer **110:**362–367. http://dx.doi.org/10.1002/ijc.20154.
27. **Toh Y, Oki E, Oda S, Tokunaga E, Ohno S, Maehara Y, Nicholson G, Sugimachi K.** 1997. Overexpression of the MTA1 gene in gastrointestinal carcinomas: correlation with invasion and metastasis. Int. J. Cancer **74:**459–463.
28. **Hofer M, Menke A, Genze F, Gierschik P, Giehl K.** 2004. Expression of MTA1 promotes motility and invasiveness of PANC-1 pancreatic carcinoma cells. Br. J. Cancer **90:**455–462. http://dx.doi.org/10.1038/sj.bjc.6601535.
29. **Toh Y, Kuwano H, Mori M, Nicolson G, Sugimachi K.** 1999. Overexpression of metastasis-associated MTA1 mRNA in invasive oesophageal carcinomas. Br. J. Cancer **79:**1723. http://dx.doi.org/10.1038/sj.bjc.6690274.
30. **Pakala SB, Singh K, Reddy SDN, Ohshiro K, Li D-Q, Mishra L, Kumar R.** 2011. TGF-β1 signaling targets metastasis-associated protein 1, a new

effector in epithelial cells. Oncogene **30:**2230–2241. http://dx.doi.org/10.1038/onc.2010.608.

31. **Zhang XY, DeSalle LM, Patel JH, Capobianco AJ, Yu D, Thomas-Tikhonenko A, McMahon SB.** 2005. Metastasis-associated protein 1 (MTA1) is an essential downstream effector of the c-MYC oncoprotein. Proc. Natl. Acad. Sci. USA **102:**13968–13973. http://dx.doi.org/10.1073/pnas.0502330102.
32. **Zhu W, Cai M-Y, Tong Z-T, Dong S-S, Mai S-J, Liao Y-J, Bian X-W, Lin MC, Kung H-F, Zeng Y-X.** 2012. Overexpression of EIF5A2 promotes colorectal carcinoma cell aggressiveness by upregulating MTA1 through C-myc to induce epithelial-mesenchymal transition. Gut **61:**562–575. http://dx.doi.org/10.1136/gutjnl-2011-300207.
33. **Yan D, Avtanski D, Saxena NK, Sharma D.** 2012. Leptin-induced epithelial-mesenchymal transition in breast cancer cells requires β-catenin activation via Akt/GSK3- and MTA1/Wnt1 protein-dependent pathways. J. Biol. Chem. **287:**8598–8612. http://dx.doi.org/10.1074/jbc.M111.322800.
34. **Hsieh AC, Liu Y, Edlind MP, Ingolia NT, Janes MR, Sher A, Shi EY, Stumpf CR, Christensen C, Bonham MJ.** 2012. The translational landscape of mTOR signalling steers cancer initiation and metastasis. Nature **485:**55–61. http://dx.doi.org/10.1038/nature10912.
35. **Ruggero D, Montanaro L, Ma L, Xu W, Londei P, Cordon-Cardo C, Pandolfi PP.** 2004. The translation factor eIF-4E promotes tumor formation and cooperates with c-Myc in lymphomagenesis. Nat. Med. **10:**484–486. http://dx.doi.org/10.1038/nm1042.
36. **Qian H, Yu J, Li Y, Wang H, Song C, Zhang X, Liang X, Fu M, Lin C.** 2007. RNA interference of metastasis-associated gene 1 inhibits metastasis of B16F10 melanoma cells in a C57BL/6 mouse model. Biol. Cell **99:**573–581. http://dx.doi.org/10.1042/BC20060130.
37. **Mizushima T, Nakagawa H, Kamberov YG, Wilder EL, Klein PS, Rustgi AK.** 2002. Wnt-1 but not epidermal growth factor induces β-catenin/T-cell factor-dependent transcription in esophageal cancer cells. Cancer Res. **62:**277–282.
38. **Huang C-L, Liu D, Ishikawa S, Nakashima T, Nakashima N, Yokomise H, Kadota K, Ueno M.** 2008. Wnt1 overexpression promotes tumour progression in non-small cell lung cancer. Eur. J. Cancer **44:**2680–2688. http://dx.doi.org/10.1016/j.ejca.2008.08.004.
39. **Kumar R, Balasenthil S, Pakala SB, Rayala SK, Sahin AA, Ohshiro K.** 2010. Metastasis-associated protein 1 short form stimulates Wnt1 pathway in mammary epithelial and cancer cells. Cancer Res. **70:**6598–6608. http://dx.doi.org/10.1158/0008-5472.CAN-10-0907.
40. **Fukuda M, Longnecker R.** 2007. Epstein-Barr virus latent membrane protein 2A mediates transformation through constitutive activation of the Ras/PI3-K/Akt Pathway. J. Virol. **81:**9299–9306. http://dx.doi.org/10.1128/JVI.00537-07.
41. **Pearce L, Alton G, Richter D, Kath J, Lingardo L, Chapman J, Hwang C, Alessi D.** 2010. Characterization of PF-4708671, a novel and highly specific inhibitor of p70 ribosomal S6 kinase (S6K1). Biochem. J. **431:**245–255. http://dx.doi.org/10.1042/BJ20101024.
42. **Li D-Q, Pakala SB, Nair SS, Eswaran J, Kumar R.** 2012. Metastasis-associated protein 1/nucleosome remodeling and histone deacetylase complex in cancer. Cancer Res. **72:**387–394. http://dx.doi.org/10.1158/0008-5472.CAN-11-2345.
43. **Reddy SDN, Pakala SB, Molli PR, Sahni N, Karanam NK, Mudvari P, Kumar R.** 2012. Metastasis-associated protein 1/histone deacetylase 4-nucleosome remodeling and deacetylase complex regulates phosphatase and tensin homolog gene expression and function. J. Biol. Chem. **287:**27843–27850. http://dx.doi.org/10.1074/jbc.M112.348474.
44. **Kumar R, Balasenthil S, Manavathi B, Rayala SK, Pakala SB.** 2010. Metastasis-associated protein 1 and its short form variant stimulates Wnt1 transcription through promoting its derepression from Six3 corepressor. Cancer Res. **70:**6649–6658. http://dx.doi.org/10.1158/0008-5472.CAN-10-0909.
45. **Moon H-E, Cheon H, Chun K-H, Lee SK, Kim Y-S, Jung B-K, Park J, Kim S-H, Jeong J-W, Lee M-S.** 2006. Metastasis-associated protein 1 enhances angiogenesis by stabilization of HIF-1α. Oncol. Rep. **16:**929–935. http://dx.doi.org/10.3892/or.16.4.929.
46. **Lin C-J, Cencic R, Mills JR, Robert F, Pelletier J.** 2008. c-Myc and eIF4F are components of a feedforward loop that links transcription and translation. Cancer Res. **68:**5326–5334. http://dx.doi.org/10.1158/0008-5472.CAN-07-5876.
47. **Gao W, Li JZH, Chan JYW, Ho WK, Wong T-S.** 2012. mTOR pathway and mTOR inhibitors in head and neck cancer. ISRN Otolaryngol. **2012:**953089. http://dx.doi.org/10.5402/2012/953089.
48. **Gulhati P, Bowen KA, Liu J, Stevens PD, Rychahou PG, Chen M, Lee EY, Weiss HL, O'Connor KL, Gao T.** 2011. mTORC1 and mTORC2 regulate EMT, motility, and metastasis of colorectal cancer via RhoA and Rac1 signaling pathways. Cancer Res. **71:**3246–3256. http://dx.doi.org/10.1158/0008-5472.CAN-10-4058.
49. **Sarbassov DD, Ali SM, Sabatini DM.** 2005. Growing roles for the mTOR pathway. Curr. Opin. Cell Biol. **17:**596–603. http://dx.doi.org/10.1016/j.ceb.2005.09.009.
50. **Bultema R, Longnecker R, Swanson-Mungerson M.** 2009. Epstein-Barr virus LMP2A accelerates MYC-induced lymphomagenesis. Oncogene **28:**1471–1476. http://dx.doi.org/10.1038/onc.2008.492.
51. **Sivendran S, Agarwal N, Gartrell B, Ying J, Boucher KM, Choueiri TK, Sonpavde G, Oh WK, Galsky MD.** 2014. Metabolic complications with the use of mTOR inhibitors for cancer therapy. Cancer Treat. Rev. **40:**190–196. http://dx.doi.org/10.1016/j.ctrv.2013.04.005.
52. **Garcia-Garcia C, Ibrahim YH, Serra V, Calvo MT, Guzman M, Grueso J, Aura C, Perez J, Jessen K, Liu Y, Rommel C, Tabernero J, Baselga J, Scaltriti M.** 2012. Dual mTORC1/2 and HER2 blockade results in antitumor activity in preclinical models of breast cancer resistant to anti-HER2 therapy. Clin. Cancer Res. **18:**2603–2612. http://dx.doi.org/10.1158/1078-0432.CCR-11-2750.
53. **O'Sullivan B, Yu E.** 2010. Staging of nasopharyngeal carcinoma, p 309–322. *In* Lee N, Kong L (ed), Nasopharyngeal cancer. Springer, New York, NY.